International Journal of Innovative
Computing, Information and Control
Volume **11**, Number **3**, June **2015**

ICIC International ©2015 ISSN 1349-4198
pp. 865–879

SHADOW DETECTION AND ELIMINATION USING A LIGHT-SOURCE COLOR VECTOR AND ITS APPLICATION TO IN-VEHICLE CAMERA IMAGES

Michio Tanaka and Takashi Morie

Graduate School of Life Science and Systems Engineering
Kyushu Institute of Technology
2-4 Hibikino, Wakamatsu-ku, Kitakyushu 808-0196, Japan
morie@brain.kyutech.ac.jp

Received August 2014; revised December 2014

Abstract. *In order to make computer vision approach human vision and to improve image recognition performance, which is often degraded by the existence of shadows, this paper proposes a new approach for shadow detection and elimination, especially for images captured by an in-vehicle camera. The proposed approach uses color vectors of regions segmented in the input image without using background information. We also propose an algorithm for automatic acquisition of the light-source color, which is required in the proposed approach, using shadow detection on a white line. The experimental results show that the success rate of shadow detection/elimination is more than 80% using the light-source color vectors, and that of shadow detection using an automatic light-source color acquisition method is about 70%. The processing time for shadow detection/elimination is less than 5 ms.*

Keywords: Shadow detection, Shadow elimination, In-vehicle camera, Color vector of light source, White line

1. **Introduction.** Significant advancement has been made in computer vision, which provides the technological basis for self-driving vehicles and autonomous intelligent robots. In some specific tasks such as human face recognition, the performance of computer vision exceeds that of humans, but in many other image-recognition tasks, computer performance is still inferior to that of humans. Shadow detection/elimination is one of these tasks. Shadows, which often exist in a natural scene image, generate boundaries or intensity changes irrelevant to the real outlines of the objects, and such boundaries affect feature extraction results and degrade object detection and recognition performance.

In order to make computer vision approach human vision, we propose a new approach of shadow detection and elimination. Although recently some feature extraction technologies have been shown to be robust to the existence of shadows [1], the performance of image recognition such as environment recognition around vehicles or robots is expected to be further improved if shadows can be explicitly detected and eliminated.

In order to detect and eliminate shadows, various approaches using background images have been proposed [2, 3, 4, 5]. In one of them, shadows are detected using such features as the color vector of a shadow in the color vector space, which can be found by extrapolating the background and environmental color vectors [3]. In this approach, a pale shadow compared with the background can be detected using the maximum allowed color shift values and minimal and maximal luminance attenuation. Another approach detects shadows using the lightness ratio and the differences in hue and saturation in the HSV color space between input and background image pixels [4]. In order to apply

these approaches to vehicle and robot vision, the background images, which are always changing, have to be estimated and updated.

Shadow detection approaches which use no background images have also been proposed [6, 7]. In these approaches, by assuming the effects of Rayleigh scattering or the features in hue values in a shadow, an original evaluation value is defined and the pixels of shadows are detected with threshold operation using Otsu's method [8]. However, these approaches were evaluated only with several images in the papers in which they were proposed; its applicability to real images in a complicated environment is not clear.

Another approach that focuses on boundaries between shadows and non-shadows was also proposed [9]. This approach also uses no background information and was not affected by the darkness of the shadows. This is based on a visual psychological model by which humans perceive a boundary where hue and luminance change simultaneously as a boundary between real objects, and one where only luminance changes as a boundary generated by a shadow. This approach is effective for shadows generated by a colorless light source, but is not so effective for those generated by a colored light source, because, in the latter case, a shadow affects hue values as well as luminance values. Moreover, in this approach, real boundaries where only luminance changes such as in black and white patterns are erroneously considered shadow boundaries.

By improving this latter approach, in this paper, we propose a new method that can achieve shadow detection/elimination without using background image. We treat images from an in-vehicle camera, in which the background image is always changing. Since the shadow includes color information of the light source, this method requires information of the light-source color before shadow detection operation. In such images, the light source is usually sunlight, but the color of sunlight changes according to the time of day and season. Therefore, since the sunlight color must be obtained periodically, we also propose an automatic acquisition method to obtain the light-source color using the white lines on the road. The proposed approach also requires a region-segmentation operation that must be performed before shadow detection. Shadows are detected using the relationship of color information between neighboring regions. This enables us to achieve a lower detection error rate compared with conventional pixel-based shadow detection approaches.

The following part of this paper is organized as follows. Section 2 describes theoretical formulation of color change on an object surface by shadow. We propose a new shadow detection/elimination method in Section 3, and an automatic acquisition method for determining light source color in Section 4. Experimental results are shown in Section 5, and we discuss the experimental results in Section 6. We conclude the paper in Section 7.

2. Theoretical Formulation of Color Change on Object Surface by Shadow.

2.1. Expression by spectral irradiance, reflectance and radiosity. Light reflects on the surface of an object and reaches the human eye, and humans can perceive the color of the object [10]. For light that a human or a camera receives through reflection off the surface of an object, this paper treats the spectra of light averaged over the whole surface of the object as follows:

$$C(\lambda) = L(\lambda)O(\lambda), \tag{1}$$

where λ is the wavelength of light, $C(\lambda)$ is the spectral radiosity averaged over the object surface, which determines the color of the object, $L(\lambda)$ is the averaged spectral irradiance of the light, and $O(\lambda)$ is the spectral reflectance of the object surface.

Let us consider a shadow as shown in Figure 1. A shadow is defined as a dark region where the light from a source is blocked. Non-shadow regions receive light from the surroundings as well as the source while shadow regions only receive light from the

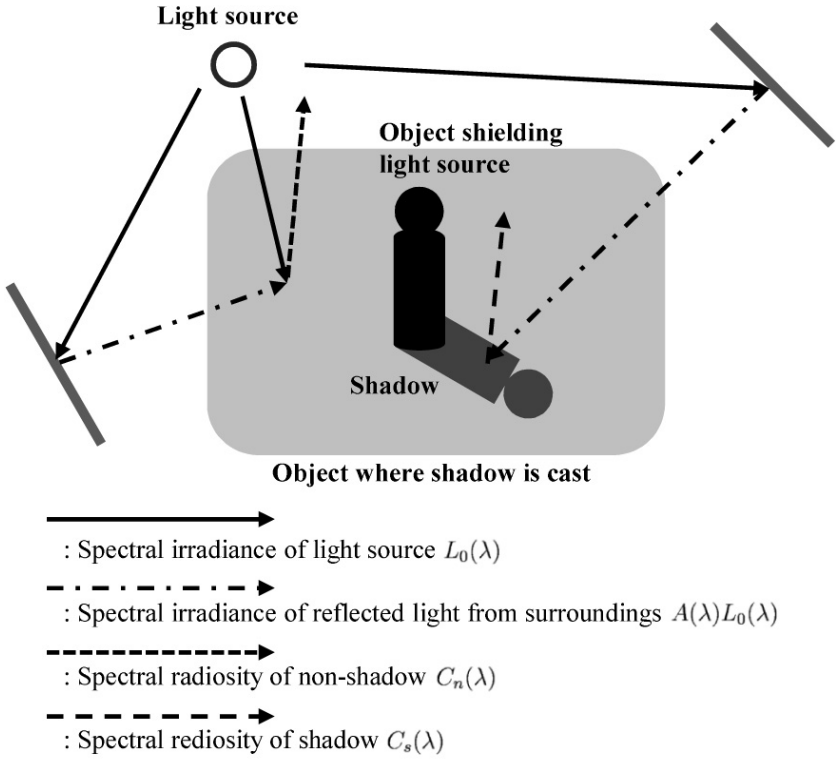

FIGURE 1. Spectral irradiance and radiosity

surroundings, which has a different spectral irradiance depending on the place. Since we treat images obtained from an in-vehicle camera, the surroundings are considered to be an open space such as on a road, and it can be assumed that no strong reflection occurs near the shadows. Therefore, the light projecting on the shadow and non-shadow regions reflected from the surroundings can be assumed to be of the same spectral pattern as the light source but with decayed irradiance. The relationship between light intensities projecting on the object is described as follows:

$$\begin{aligned} L_n(\lambda) &= L_0(\lambda) + pA(\lambda)L_0(\lambda), \\ L_s(\lambda) &= qA(\lambda)L_0(\lambda), \end{aligned} \tag{2}$$

where $L_n(\lambda)$ and $L_s(\lambda)$ are averaged spectral irradiances projecting on non-shadow and shadow regions, respectively, and $L_0(\lambda)$ is the average spectral irradiance of the light source. Light reflected from the surroundings can be expressed by the source light decayed per decay constant $A(\lambda)$. This decay constant changes depending on the place at non-shadow or shadow regions; this change is expressed by constants p and q.

From the above formulation, the change in the color of the object surface by a shadow is represented as follows:

$$\begin{aligned} C_d(\lambda) &= C_n(\lambda) - C_s(\lambda) \\ &= O(\lambda)(L_n(\lambda) - L_s(\lambda)) \\ &= O(\lambda)(L_0(\lambda) + (p-q)A(\lambda)L_0(\lambda)) \\ &= C_0(\lambda) + rC_s(\lambda), \end{aligned} \tag{3}$$

$$r = (p-q)/q, \tag{4}$$

where $C_n(\lambda)$ and $C_s(\lambda)$ are average spectral radiosities on non-shadow and shadow regions, respectively, $C_d(\lambda)$ is the difference between them, and $C_0(\lambda)$ is formally defined as $O(\lambda)L_0(\lambda)$, which is determined only by the light source. Constant r is the difference between the reflection light intensities on the shadow and non-shadow regions.

2.2. **Expression by color vectors.** Based on the characteristics of perception in the human visual system, light spectra can be expressed by a color vector $\mathbf{v}$ in the color space using a color-matching function $\mathbf{M}$:

$$\mathbf{v} = \mathbf{M}C(\lambda). \tag{5}$$

The shape and intensity of the spectrum affect the angle and length of the color vector, respectively.

Using Equations (3) and (5), the change of the color vector by a shadow is expressed as follows:

$$\begin{aligned} \mathbf{v}_d &= \mathbf{v}_n - \mathbf{v}_s \\ &= \mathbf{v}_0 + r\mathbf{v}_s, \end{aligned} \tag{6}$$

where $\mathbf{v}_d$, $\mathbf{v}_n$, $\mathbf{v}_s$, and $\mathbf{v}_0$ are the color vectors corresponding to $C_d(\lambda)$, $C_n(\lambda)$, $C_s(\lambda)$, and $C_0(\lambda)$, respectively.

On the same object surfaces, the color vectors of shadow $\mathbf{v}_s$ are parallel. Here, we define $\hat{\mathbf{v}}_s$ as a normalized color vector of the shadow that is arbitrarily chosen from vectors $\mathbf{v}_s$ beforehand. Specifically, from images captured in the environment with the same $L_0(\lambda)$ and $A(\lambda)$, we can obtain $\hat{\mathbf{v}}_s$ manually or by detecting shadows with an appropriate method, without measuring $L(\lambda)$, $A(\lambda)$, and $O(\lambda)$.

Regarding shadows on a different object, because $O(\lambda)$ is different, color vectors change as shown in Figure 2(b); the new color vectors are defined as $\mathbf{v}'_d$, $\mathbf{v}'_n$, $\mathbf{v}'_s$, and $\hat{\mathbf{v}}'_s$, and a compensation operation is required to apply $\hat{\mathbf{v}}_s$ that was obtained in the different surface. Since shadows in vehicle vision are generated at places such as roads, sidewalks, and road sign regions, $O(\lambda)$ is not so different, and it can be assumed that the difference in $\hat{\mathbf{v}}_s$ is expressed by $\mathbf{v}'_n$. By using $\mathbf{v}'_n$ and the following transformation matrix $\mathbf{F}$, vector $\mathbf{F}\mathbf{v}'_n$ that compensates for $\hat{\mathbf{v}}'_s$ is calculated, as shown in Figure 2(b). By including $\mathbf{F}\mathbf{v}'_n$, the difference in $O(\lambda)$ is compensated as follows:

$$\hat{\mathbf{v}}_s \parallel \mathbf{F}\mathbf{v}'_n + \hat{\mathbf{v}}'_s, \tag{7}$$

where $\mathbf{v}'_n$ and $\mathbf{v}'_s$ are color vectors of non-shadow and shadow regions on object surfaces different from those on which $\hat{\mathbf{v}}_s$ was calculated.

These color changes are calculated by addition/subtraction, and an *opposite color space* with an orthogonal coordinate system is suitable for their calculation. The opposite color space is used in the human visual system and consists of hue axes (red-green axis, yellow-blue axis) and a luminance axis. We can easily convert the *RGB color space* obtained by an image sensor into the opposite color space (Figure 3). Therefore, the color vector $\mathbf{v}$ is expressed as follows:

$$\mathbf{v} = \begin{pmatrix} v_r \\ v_y \\ v_l \end{pmatrix}, \tag{8}$$

where v_r, v_y and v_l are intensities of red/green, yellow/blue and luminance, respectively. Since the opposite color space has three dimensions, $\mathbf{F}$ is a square matrix with three rows

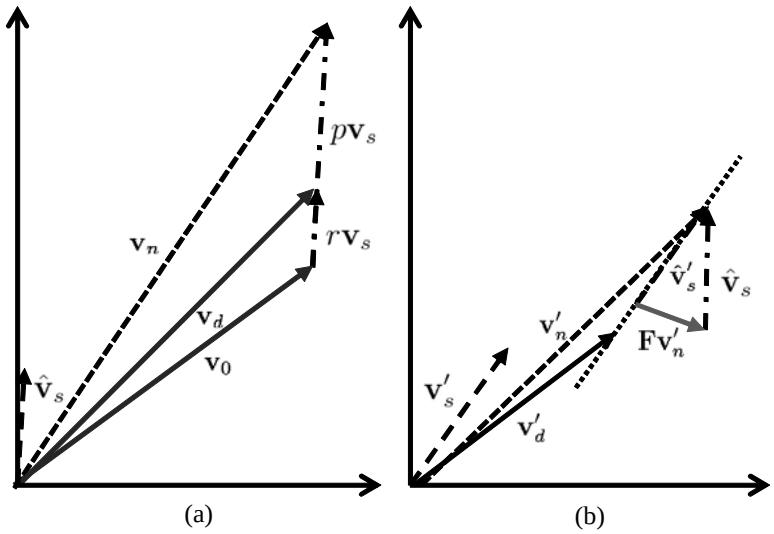

FIGURE 2. Relationships between color vectors of non-shadow and shadow regions in a color space: (a) the basic concept shown in Equation (6), and (b) compensation of $\hat{\mathbf{v}}'_s$ shifted by the difference of object surfaces where a shadow is cast by $\mathbf{F}\mathbf{v}'_n$, as shown in Equation (7)

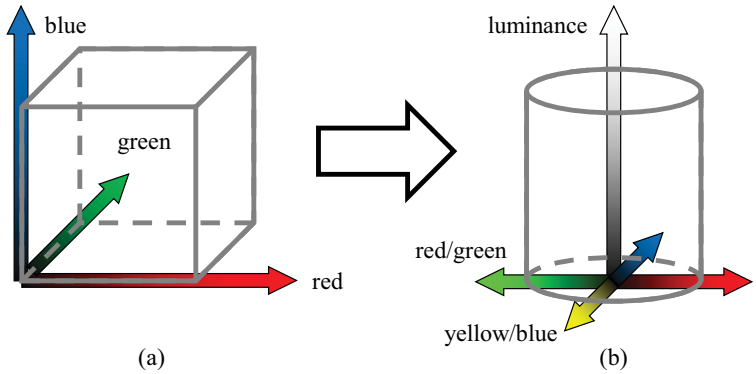

FIGURE 3. Color spaces: (a) RGB color space, and (b) opposite color space

and columns:

$$\mathbf{F} = \begin{bmatrix} F_{0,0} & F_{0,1} & F_{0,2} \\ F_{1,0} & F_{1,1} & F_{1,2} \\ F_{2,0} & F_{2,1} & F_{2,2} \end{bmatrix}. \tag{9}$$

3. **Shadow Detection/Elimination Method.** We detect a shadow by comparing the colors of neighboring regions obtained by region segmentation. The flowchart of shadow detection and elimination is shown in Figure 4.

First, we perform region segmentation of the input image. In this paper, region segmentation was achieved by combining edge detection and labeling. Other methods can be used, such as the mean shift method and clustering [11, 12].

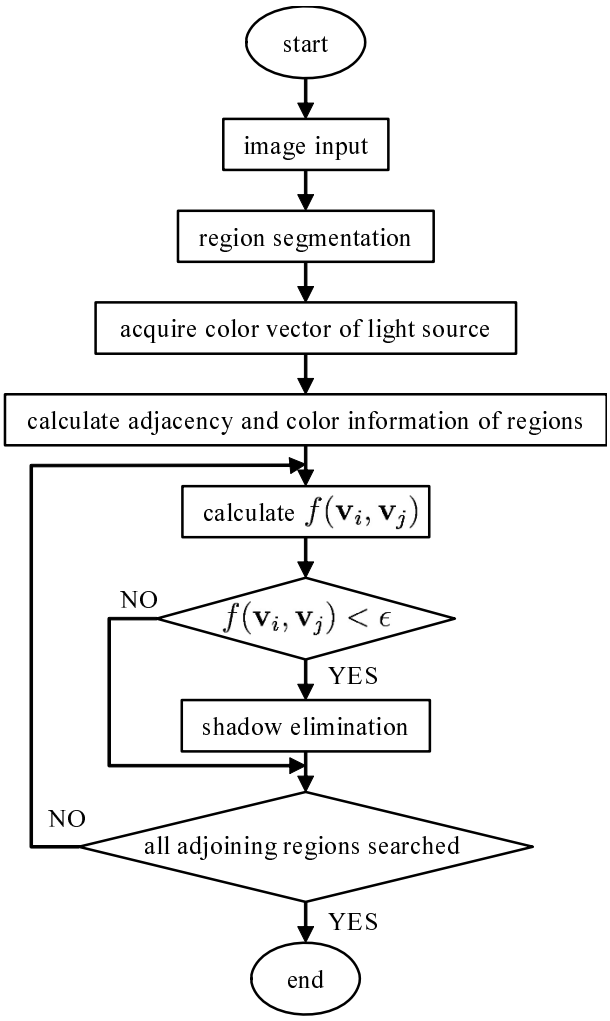

FIGURE 4. Flowchart of shadow detection and elimination

Next, based on Equation (7), we evaluate function $f(\mathbf{v}_i, \mathbf{v}_j)$, which is defined by the color vectors of neighboring regions:

$$f(\mathbf{v}_i, \mathbf{v}_j) = 1 - \frac{< \hat{\mathbf{v}}_s, \mathbf{F}\mathbf{v}_i + \hat{\mathbf{v}}_j >}{\|\hat{\mathbf{v}}_s\| \|\mathbf{F}\mathbf{v}_i + \hat{\mathbf{v}}_j\|}, \tag{10}$$

where $\mathbf{v}_i$ and $\mathbf{v}_j$ are color vectors of arbitrary neighboring regions. It is noticed that $\hat{\mathbf{v}}_s$ and $\mathbf{F}$ have to be acquired beforehand, and are affected by the spectral reflectance of the source light and the object surface where shadows are cast, respectively. According to Equation (7), if $f(\mathbf{v}_i, \mathbf{v}_j) < \epsilon$, then $\mathbf{v}_i$ and $\mathbf{v}_j$ are considered as $\mathbf{v}_n$ and $\mathbf{v}_s$, respectively, where ϵ is a threshold.

Finally, the detected shadow is eliminated by adding $\mathbf{v}_d$ to the whole shadow region based on Equation (6).

4. **Automatic Acquisition of Color of Light Source.** As described in the previous section, it is necessary to obtain the color vector of the light source $\hat{\mathbf{v}}_s$ before performing shadow detection and elimination operation. If we know $\mathbf{v}_n$ and $\mathbf{v}_s$, the color vector of the light source can be obtained from Equation (6). In order to achieve that, the colors of the object regions have to be known. Here, we propose an automatic acquisition technique of the color of the light source. This technique uses white line regions that exist on most of

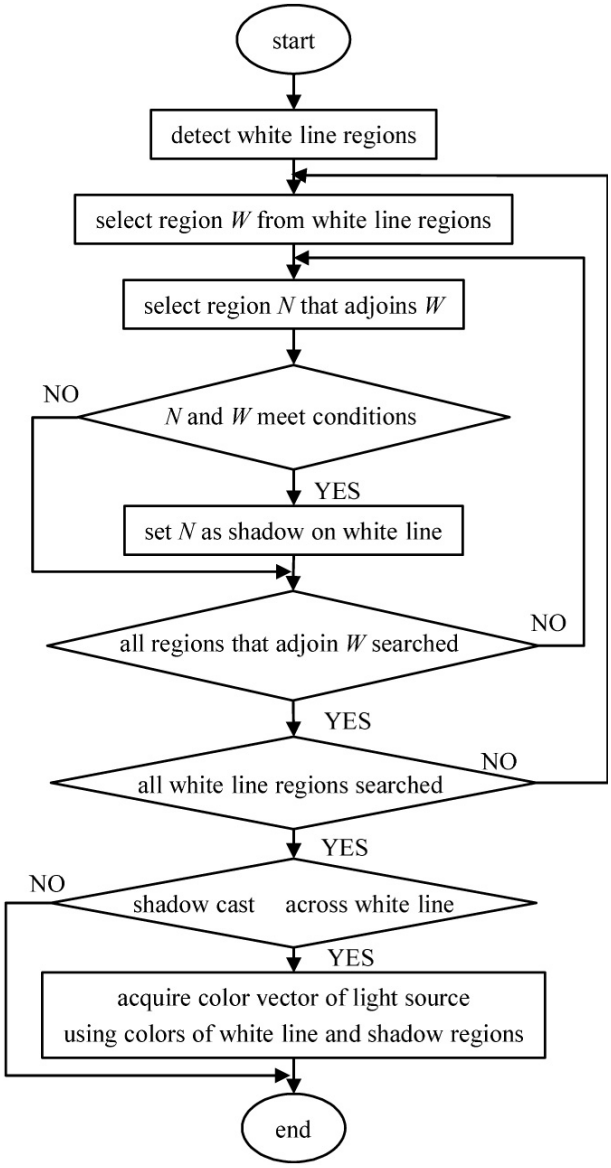

FIGURE 5. Flowchart of automatic acquisition of the color of the light source

all road surfaces in Japan. The flowchart of the automatic acquisition of the color of the light source is shown in Figure 5.

First, we detect a white line region in the image obtained from an in-vehicle camera. White line detection is relatively easy, and various techniques have been proposed. The technique proposed here uses the region color, the position and the shape of a white line; such characteristics are stable because they are provided by the road traffic law in Japan. The procedure is as follows.

1. Perform region segmentation in an image obtained from an in-vehicle camera.
2. Choose white regions from segmented regions based on v_l. The luminance v_l of white regions is required to be above the predefined threshold value.
3. Search vertically long regions based on the predefined aspect ratio because a white line in an in-vehicle camera image is a vertically long and slender rectangle.
4. Identify a white line by restricting the position; that is, on the road surface and on both sides of the lanes.

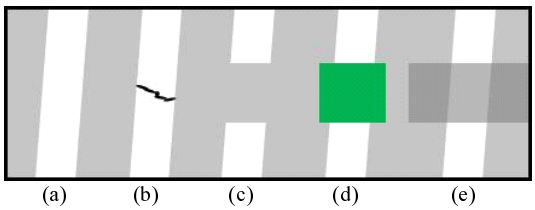

FIGURE 6. States of white line: (a) white line only, (b) grime on a white line, (c) gap in a white line, (d) object on a white line, (e) shadow cast across a white line

Next, we detect the shadow region on the white line by using the relationship between the white line and its adjacent region. We classify the condition of a white line into five situations, as shown in Figure 6. For a white line only (Figure 6(a)) or for grime on the white line (Figure 6(b)), the white line is not split by non-white regions with a meaningful size although the grime may split the white line by a narrow non-white region. For a gap in the white line (Figure 6(c)) or for an object on the white line (Figure 6(d)), the white line is broken off. In these cases, even if the white-line region adjoins the non-white region, these side edges are not on the same straight line. When the shadow is on the white line (Figure 6(e)), not only shadow edges but also white line edges remain. This means that a shadow region on the white line adjoins the white-line regions, and these edges are on the same straight line. Using these conditions, we can detect a shadow region on the white line. Once we detect a shadow on the white line, the color of the light source can be obtained from the difference of colors of the shadow and the white-line regions.

5. **Experiments.**

5.1. **Experimental conditions and evaluation method.** The performances of two operations, automatic acquisition of the light-source color and shadow detection/elimination, were evaluated. The experiments used images of the front scenes from a vehicle captured by an in-vehicle camera.

Before the evaluation experiments for shadow detection/elimination, we performed an experiment for acquiring $\mathbf{F}$. We used test images that included road surfaces and white lines with shadow regions, selected the shadow regions manually in the test images, and obtained $\mathbf{v}_n$ and $\mathbf{v}_s$, where $\hat{\mathbf{v}}_s$ was assumed to be acquired using shadows on the white lines. Based on Equation (10), $f(\mathbf{v}_n, \mathbf{v}_s)$ was calculated for all pairs of $\mathbf{v}_n$ and $\mathbf{v}_s$, and the optimum $\mathbf{F}$ was obtained so as to minimize the total of $f(\mathbf{v}_n, \mathbf{v}_s)$. Here, $\hat{\mathbf{v}}_s$ was obtained using $\mathbf{v}_s$ on the white-line region.

In the experiments for light-source color vector acquisition using white lines, 40 images were used where shadows were on the white-line region. This set of images was the same as that used for obtaining $\mathbf{F}$. We defined the evaluation value η_w as follows:

$$\eta_w = \frac{TP_l}{TP_l + FN_l} \tag{11}$$

where TP_l and FN_l are the number of pixels of shadow regions on the white line with successful detection and that with failed detection, respectively.

The accuracy of shadow region detection was evaluated based on the successful shadow-detection rate. Ground-truth data were obtained by manually discriminating shadow and non-shadow regions. The test data were 88 consecutive images, and η was defined as

TABLE 1. Methods for evaluation experiments of shadow detection

	$\hat{\mathbf{v}}_s$	$\mathbf{F}$
(1)	manual acquisition using shadow on the road	not used
(2)	automatic acquisition using shadow on the white line	not used
(3)	automatic acquisition using shadow on the white line	used

follows:

$$\eta = \frac{TP_s}{TP_s + FN_s} \tag{12}$$

where TP_s and FN_s are the number of pixels of shadow regions with successful detection and failed detection, respectively.

Although there are some paved road surfaces, if values of $O(\lambda)$ on roads are not so different, the shadows on a road surface should be able to be detected accurately even with $\hat{\mathbf{v}}_s$ obtained on a different road surface instead of using $\mathbf{F}$. However, because it is difficult to detect shadows on a road without $\hat{\mathbf{v}}_s$, we proposed an automatic shadow detection method on a white line using boundary features, as shown in Section 4. Thus, we performed experiments under three methods as shown in Table 1, where the same set of images was used to obtain $\hat{\mathbf{v}}_s$. In order to compare our approach with conventional ones, we implemented the approaches proposed in Refs. [6] and [7], and applied them to the same test images.

In the shadow elimination experiment, we used the same images as in the shadow detection experiment, and calculated the elimination rate by counting the number of images in which the shadow regions were eliminated by a region-segmentation processing after shadow elimination.

5.2. **Experimental results.** The experimental results for distribution of $\mathbf{v}_s$ are shown in Figure 7, which was used for obtaining $\mathbf{F}$. The color vectors $\mathbf{v}_s$ for shadows on white lines and those for shadows on roads are on different straight lines. It was found from these results that the compensation by $\mathbf{F}\mathbf{v}_n$ shown in Figure 2(b) is feasible. We obtained $\mathbf{F}$ as follows, and used it in the experiments for the performance evaluation of shadow detection.

$$\mathbf{F} = \begin{bmatrix} -16.000000 & -61.298388 & 113.933105 \\ -8.000000 & 8.912572 & 68.822290 \\ 32.000000 & -35.558340 & -275.262606 \end{bmatrix} \tag{13}$$

A shadow detection result on a road including a white line is shown in Figure 8. Figure 8(b) shows the segmentation result, and the shadow region on the white line in Figure 8(c) is indicated by the gray region. Figure 8(d) shows shadow regions including a shadow on the white line detected based on the light-source color obtained using the automatic acquisition method. Another shadow detection result on a road with the same parameters as those used in Figure 8 is shown in Figure 9. The successfully detected shadow region is shown in Figure 9(c).

The rates of successful shadow detection are shown in Table 2. From this table, both shadows on the roads in method (1) and those on surfaces other than roads in method (2) were successfully detected. This means that the orientations of all measured $\mathbf{v}_s$ on roads were nearly the same, and those on surfaces other than roads were also the same, which corresponds to the results shown in Figure 7. It is also seen from Table 2 that

TABLE 2. Successful detection rates in shadow detection experiments

target	method (1)	method (2)	method (3)	Ref. [6]	Ref. [7]
shadows on roads	89.2%	0.0%	86.1%	92.9%	93.4%
shadows on surfaces other than roads	0.0%	81.6%	77.2%	37.4%	56.5%
all shadows	63.2%	23.8%	83.4%	77.6%	83.2%

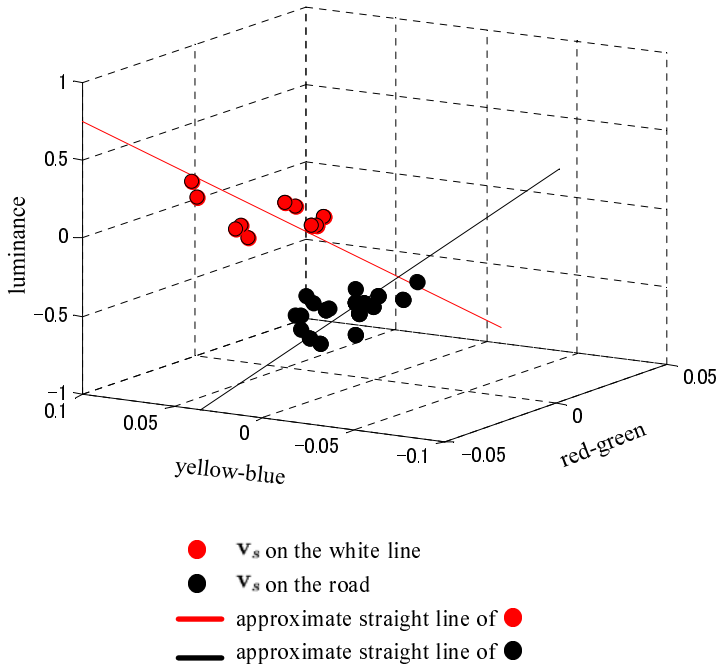

FIGURE 7. Distribution of $\mathbf{v}_s$ used for obtaining $\mathbf{F}$

shadows on surfaces other than roads in method (1) and those on roads in method (2) cannot be detected, but 80% of all shadows can be detected in method (3). This proves the effectiveness of $\mathbf{F}$. Table 2 also shows the success rates in the conventional methods proposed in Refs. [6] and [7]. The obtained results are compared and discussed in the next section.

Shadow elimination results are shown in Figures 10 and 11. The region segmentation results using these results are shown in (d) in each figure.

The success rate of shadow detection on a white line, η_w, was 87.5%. Figure 12 shows a misdetection result, where a part of the white line was misdetected as a shadow. This error was caused by misdetection of the white-line region due to the luminance change by a stain on the white line. However, improved white-line detection techniques have already been established, and misdetection of white lines can be avoided using such established techniques.

6. **Discussion.** The proposed approach has nearly the same rate of successful detection for total shadow regions as the conventional approaches, as shown in Table 2. In addition, for shadows on surfaces other than roads, the proposed approach has a much better detection rate. One example of shadow detection results is shown in Figure 13, where method (3) successfully detected only shadow regions, whereas the conventional approaches detected a paved surfaced road and trees. This is due to the difference of types of color

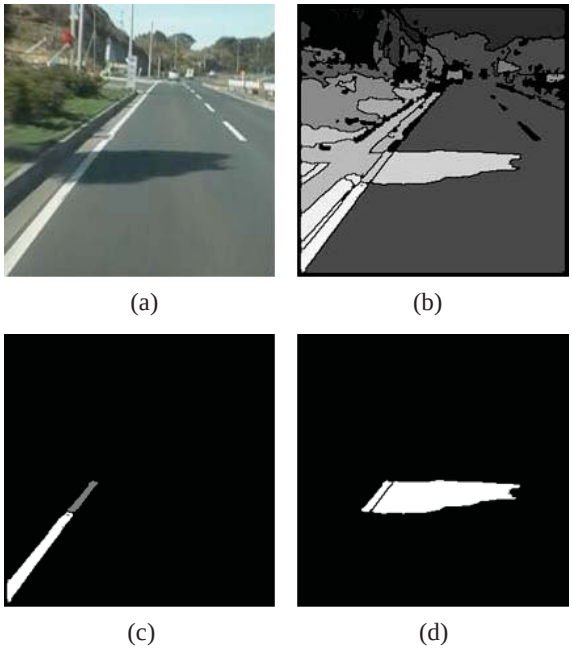

FIGURE 8. Shadow detection result on a white line: (a) input image, (b) region segmentation result, (c) detection result of a shadow on the white line, (d) shadow detection result using light-source color obtained using the proposed automatic acquisition technique

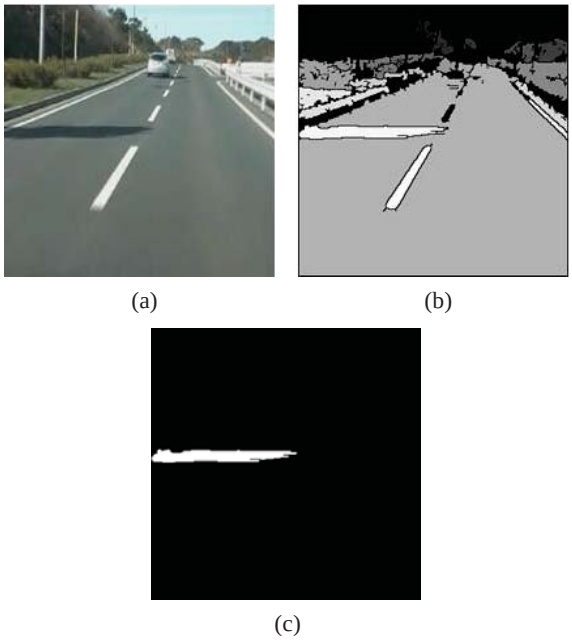

FIGURE 9. Shadow detection result: (a) input image, (b) region segmentation result, (c) shadow detection result

information and the targeted regions used in the proposed and conventional approaches. The conventional approaches used two types of color information in a pixel for shadow detection: hue and luminance were used in Ref. [6], and saturation and luminance were used in Ref. [7]. On the other hand, the proposed approach uses three types of color information and the relationship of color vectors between neighboring regions instead of

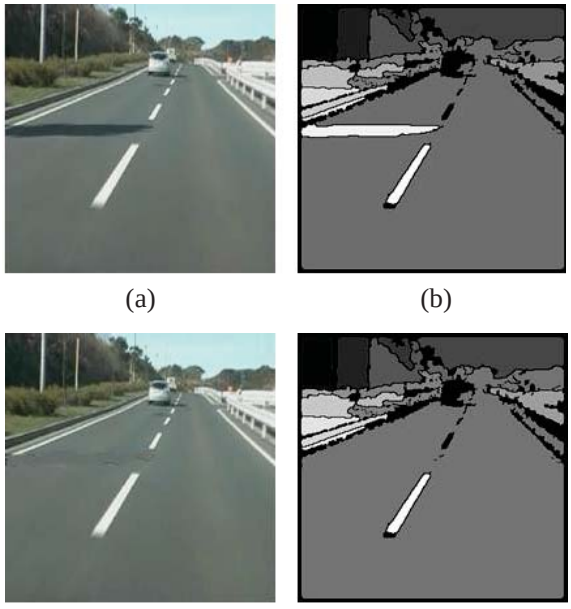

FIGURE 10. Shadow elimination result (1): (a) input image, (b) region segmentation result, (c) shadow elimination result, (d) region segmentation result using the shadow elimination result

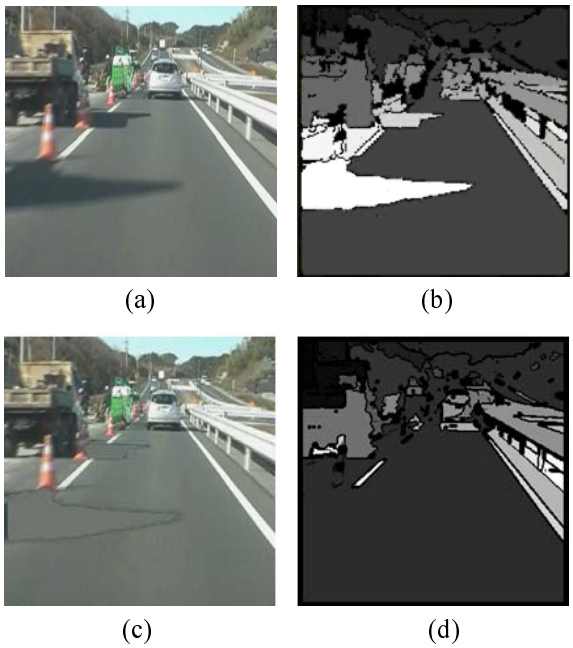

FIGURE 11. Shadow elimination result (2): (a) input image, (b) region segmentation result, (c) shadow elimination result, (d) region segmentation result using the shadow elimination result

pixels. Thus, the proposed approach uses more information and leads to a decrease in the rate of failed detection.

The proposed approach detects shadows by comparing the angle between the color vectors of neighboring regions with a predefined threshold value, as described in Section 3.

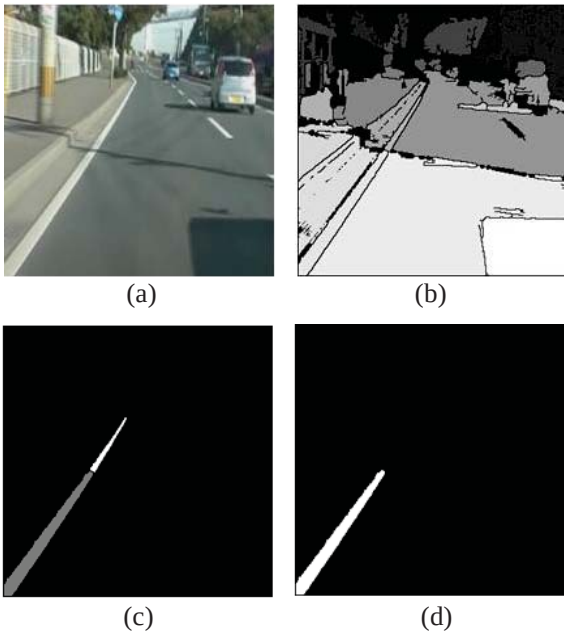

FIGURE 12. Misdetection result of shadows on a white line: (a) input image, (b) region segmentation result, (c) detection result of a shadow on the white line, (d) shadow detection result using light-source color obtained using the proposed automatic acquisition technique

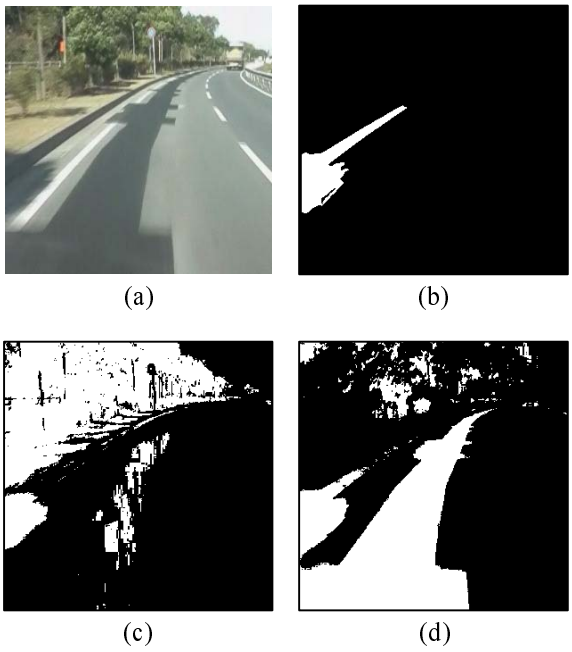

FIGURE 13. Comparison result of shadow detection: (a) input image, (b) result of method (3), (c) result in HSV of Ref. [6], (d) result of Ref. [7]

However, such evaluation based on only one item often leads to misdetection due to noise. In order to improve the performance, new evaluation items for detection are required. For example, as the white-line contours shown in Figure 6(e), we could use the fact that the object contours remain even when shadows are cast.

In shadow elimination experiments, we were able to remove all the shadow regions from the segmented regions after shadow elimination. The proposed approach introduces almost no effects of shadows to the post-processing, as shown in Figure 10(c). However, the boundary contours of the shadows remain in some experimental results, as shown in Figure 11(c). This is due to gradual changes of the intensity at the boundaries of shadows depending on the surroundings and the shielding objects, which are leaves of trees lining a street in this case. Since leaves at branches of trees have less density at the periphery than at the center, more light penetrates at the periphery and the boundary of the shadow is brighter. Because of such local color changes, some shadow regions cannot be segmented. This problem could be solved by improving the region segmentation method. In shadow elimination processing, since the same value was added to the whole shadow region in this experiment, the boundaries of the shadows became brighter. This can be improved by modifying the addition value depending on the color vector change in the shadow region.

7. **Conclusion.** We proposed a shadow detection/elimination approach that uses color vectors of regions segmented in the input image without using background information. It was verified from experimental results that automatic light-source color acquisition using shadow detection on a white line and shadow detection/elimination were successfully achieved. The success rate of shadow detection/elimination was more than 80% using light-source color vectors, and that of shadow detection using automatic light-source color acquisition was about 70%. The processing time for shadow detection/elimination was less than 5 ms.

Since the performance of the proposed approach strongly depends on that of image region segmentation, segmentation methods more suitable to this approach should also be developed. In the future we will apply our method to more complicated shadow patterns such as that made by sunlight filtering through tree leaves.

We mainly assumed vehicular environments such as road surfaces in this paper, but as long as the assumed conditions are satisfied, the proposed approach can also be valid. In future works, we will apply the proposed approach to images in other environments by setting $\mathbf{F}$ appropriately. Possible applications of our shadow detection/elimination are in satellite/aerial photographs and autonomous moving robot vision, where obtaining an accurate background image is difficult.

Acknowledgment. The authors gratefully acknowledge the helpful comments and suggestions of Prof. Zdenek Prochazka.

REFERENCES

[1] D. G. Lowe, Object recognition from local scale-invariant features, *Proc. of IEEE Int. Conf. on Computer Vision (ICCV)*, pp.1150-1157, 1999.

[2] A. J. Joshi and N. Papanikolopoulos, Learning of moving cast shadows for dynamic environments, *2008 IEEE Int. Conf. on Robotics and Automation (ICRA'08)*, pp.987-992, 2008.

[3] J. B. Huang and C. S. Chen, Moving cast shadow detection using physics-based features, *The 2nd Int. Cong. on Image and Signal Processing (CISP'09)*, pp.1-5, 2009.

[4] H. Liu, C. Yang, X. Shu and Q. Wang, A new method of shadow detection based on edge information and HSV color information, *The 2nd Conf. on Power Electronics and Intelligent Transportation System (PEITS'09)*, pp.286-289, 2009.

[5] J. Gao, H. Zhang and Y. Liu, Foreground and shadow segmentation by exploiting multiple cues, *Proc. of the 10th ACIS Int. Conf. on Software Engineering, Artificial Intelligences, Networking and Parallel/Distributed Computing (ANPD'09)*, pp.286-289, 2009.

[6] V. J. D. Tsai, A comparative study on shadow compensation of color aerial images in invariant color models, *IEEE Trans. Geoscience and Remote Sensing*, vol.44, no.6, pp.1661-1671, 2006.

[7] K. K. Singh, K. Pal and M. J. Nigam, Shadow detection and removal from remote sensing images using NDI and morphological operators, *Int. J. Computer Applications*, vol.42, no.10, pp.37-40, 2012.
[8] N. Otsu, A threshold selection method from gray-level histograms, *IEEE Trans. Systems, Man and Cybernetics*, vol.9, no.1, pp.62-66, 1979.
[9] T. Kamada, A. Hanazawa and T. Morie, Shadow elimination mimicking the human visual system, *Brain-Inspired Information Technology (Studies in Computational Intelligence)*, pp.147-151, 2009.
[10] D. A. Forsyth and J. Ponce, Computer vision: A modern approach, *Prentice Hall Professional Technical Reference*, 2002.
[11] M. Carreira-Perpinan, Gaussian mean-shift is an EM algorithm, *IEEE Trans. Pattern Analysis and Machine Intelligence*, vol.29, no.5, pp.1160-1167, 2006.
[12] X. T. Yuan, B. G. Hu and R. He, Agglomerative mean-shift clustering, *IEEE Trans. Knowledge and Data Engineering*, vol.24, no.2, pp.209-219, 2012.